# Supporting Information

## Succulent Inspired Grown g-$C_3N_4$@Lithium Sodium Niobate for Supercapacitor and Piezo-Tuned Electrochemical Potential Controlled Smart Electromagnetic Shielding Management

Prem Pal Singh, Bhanu Bhusan Khatua*

Materials Science Centre, Indian Institute of Technology Kharagpur, Kharagpur -721302, India.

*Corresponding author-

Prof. B. B. Khatua (Email: khatuabb@matsc.iitkgp.ac.in)

Materials Science Centre, Indian Institute of Technology Kharagpur, Kharagpur - 721302, India

Tel.: +91- 3222-283982

## 1. TGA analysis of LNN and GNLNN

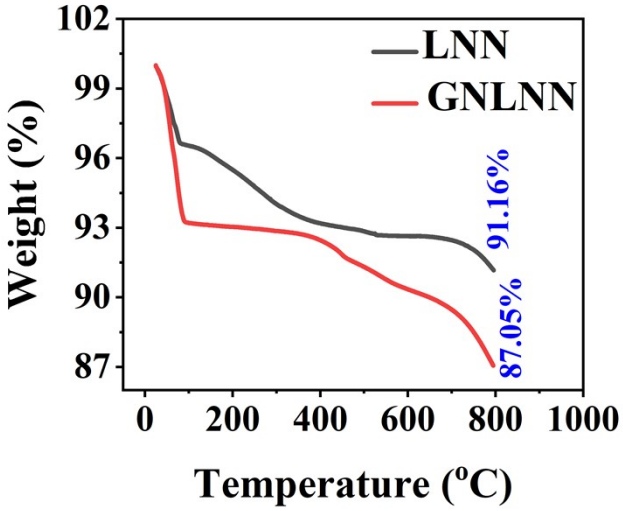


Fig. S1. TGA analysis of LNN and GNLNN nanoparticles.

## 2. Uv-Vis analysis of LNN and GNLNN

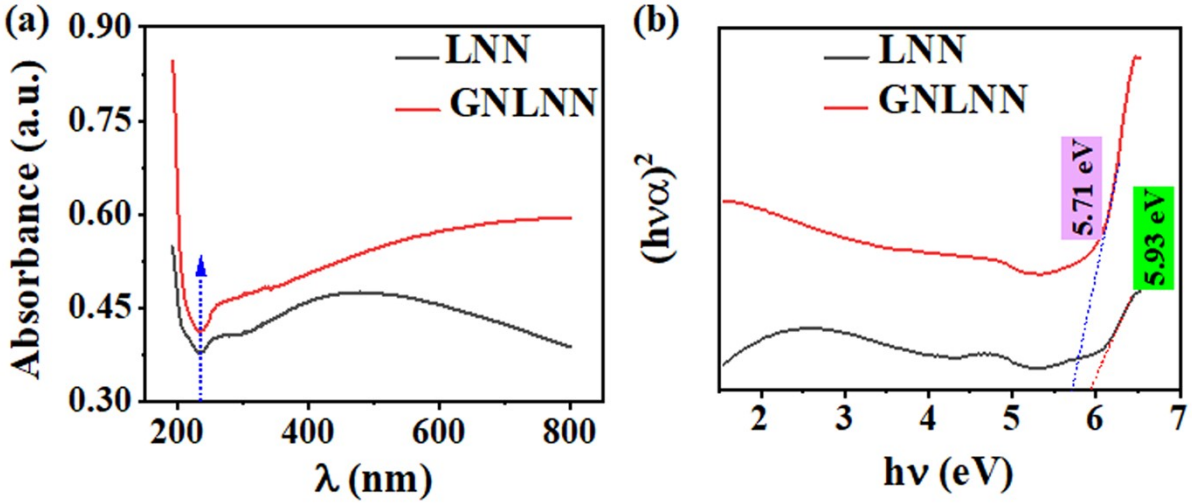


Fig. S2. (a) UV–visible absorption spectra of LNN and GNLNN, (b) Tacu's plot of LNN and GNLNN.

## 3. EDS mapping of GNLNN

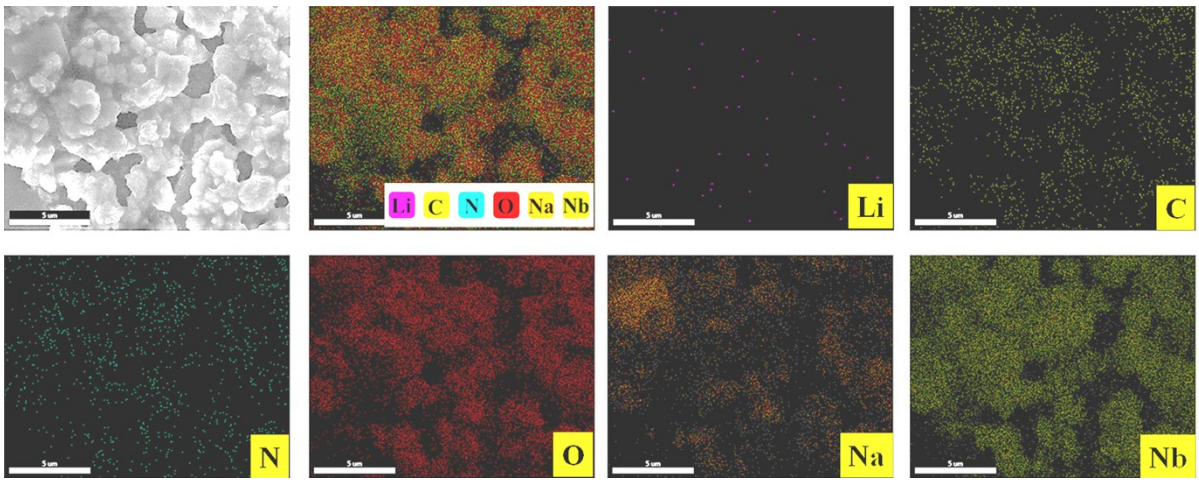


Fig. S3. EDS elemental mapping of GNLNN.

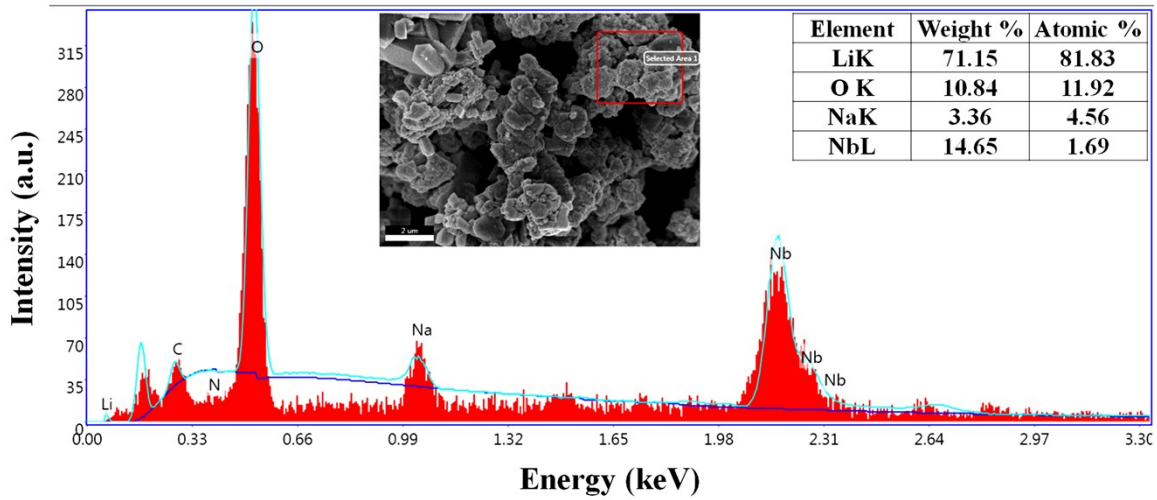


Fig. S4. EDS elemental spectra of LNN nanoparticles.

**Table S1.** Summary of peak positions of individual elements in LNN and GNLNN from XPS spectra.

| Elements | LNN (Peak Position, in eV) | GNLNN (Peak Position, in eV) | B.E. Shift (eV) |
|---|---|---|---|
| **Li 1s** | 54.5 | 55.7 | + 1.18 |
| **C 1s** | - | 284.76 | |
| | - | 288.4 | |
| **N 1s** | | 398.79 | |
| | | 399.9 | |
| **O 1s** | 529.2 | 529.7 | + 0.5 |
| | 530.85 | 531.3 | + 0.45 |
| **Na 1s** | 1070.6 | 1072.1 | + 1.5 |
| **Nb 3d** | 206.19 | 206.79 | + 0.6 |
| | 208.94 | 209.55 | + 0.61 |

## 4. Used equations

### 4.1. Specifirc capactiance form CV meaurements[1]

$$C_s = \frac{2\int IdV}{m\nu\Delta V} \tag{1S}$$

Where I(A) is the current, V(V) is potential, ν is the scanning rate (mV/s), m is the amount of active mass loading (g), and ΔV is the potential window.

### 4.2. Specific capacitance calculation from the GCD curves[1]

$$C_s = \frac{2Idt}{mdV} \tag{2S}$$

Where, I/m is the current density (A/g), dt is the discharge time, and dV is the potential drop during the discharging process (in V).

### 4.3. Device parameters from GCD measurements[2,3]

$$Device\,Capaci\tan ce\,(C_d) = \frac{4Idt}{mdV} \tag{3S}$$

$$Specific\,Energy\,(E_{sp}) = \frac{C_d(\Delta V)^2}{7.2} \tag{4S}$$

$$Specific\,Power\,(P_{sp}) = \frac{3600 \times E_{sp}}{\Delta t} \tag{5S}$$

$$Coulombic\,Efficiency(\eta) = \frac{\Delta t}{\Delta t_c} \tag{6S}$$

Where Δt is the discharge time (s), $\Delta t_c$ is the charging time (s).

### 4.4. Randles–Sevcik equation[4]

$$D = \left[\frac{i}{2.69\times10^5 \times n^{3/2} \times \nu^{1/2} \times C \times A}\right]^2 \tag{7S}$$

Where i is current (Amp), n is the electrons transferred during redox reaction, C is the concentration of electrolyte, A is the active surface area ($cm^2$), ν is the scan rate (V/s).

## 5. Diffusion coefficients of LNN and GNLNN

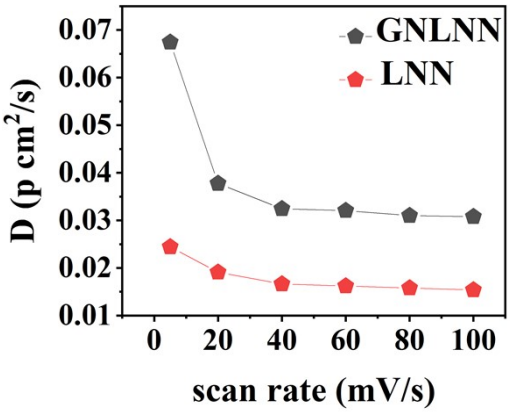


Fig. S5. Diffusion coefficients at varying scan rates of LNN and GNLNN.

## 6. Electrochemical (GCD) cyclic stability of GNLNN and device

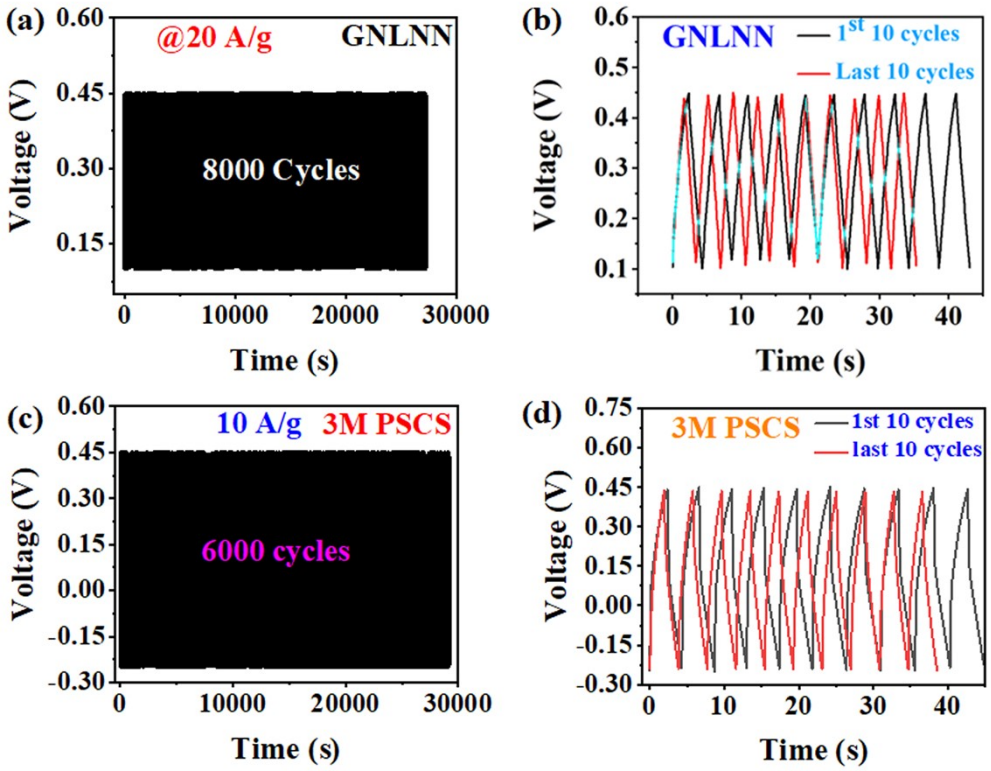


Fig. S6. (a) charging-discharging stability of GNLNN electrode for 5000 GCS cycles, (b) 1st initial 10 charging-discharging cycles and last 10 charging-discharging cycles during GCD analysis of GNLNN electrodes, (c) charging-discharging stability of 3M PSCS device for 5000 cycles, (d) 1st initial 10 charging-discharging cycles and last 10 charging-discharging cycles during GCD analysis of 3M PSCS device.

## 7. Finger imparting force calculation

A physical model consisting of the gravity term and pulse term was adopted to calculate the imparting pressure. When an object (finger) falls on the composite, it should comply with the main criteria: (i) first, it should touch the surface, and (ii) it should complete the action on the surface of the composite. Hence, based on the momentum and kinetic energy theorem, the following equations could be introduced.[6]

$$m.g.h = \frac{1}{2}m.V^2 \quad (8S)$$

$$(F - m.g).\Delta t = mV \quad (9S)$$

$$\sigma = \frac{F}{A} \quad (10S)$$

Where m is the mass of the object (finger) (kg), h is the height of mass falling (in meters), σ is the applied mechanical pressure, V is the maximum falling velocity (m/s), F is the contact force, and Δt is the time span. Approximate applied pressure values are calculated by inserting calibrated and measured values data.

## 8. Electromagnetic theory of self-charging

The electromagnetic theory can be applied to explain the self-charging mechanism. Prior to the application of pressure, the 3M PSCS device adheres to the principle of energy conservation, indicating that the total power on charges may be determined by integrating the flow of energies from the surface (S) of the system of volume (V) per unit time (t). Thus, equation (11S) is employed to compute the net energy flow in the composite.[5,6]

$$-\iiint \vec{f}.\vec{v}\,dV = \hat{x}\oiint \vec{S}\,d\vec{\sigma} + \frac{d}{dt}\iiint \omega\,dV \quad (11S)$$

The symbol S represents the flux density, whereas the symbol ω ( $= \frac{\vec{E}.\vec{D}}{2} + \frac{\vec{H}.\vec{B}}{2}$ ) represents the total energy density of the electromagnetic field in closed volume. When the 3M PSCS device gets subjected to external pressure, a point comes where the pressure surpasses the electromagnetic and elastic forces already present in the PSCS device. Now, the rate of energy density can be written as,

$$\frac{\partial \omega}{\partial t} = \vec{E}.\frac{\partial \vec{D}}{\partial t} + \vec{H}.\frac{\partial \vec{B}}{\partial t} \tag{12S}$$

The work used to counteract the elastic energy results in a modification of the elastic potential energy (EPE) and polarization energy (PE) within the material, leading to the formulation of equation (13S).

$$P - \oiint \vec{S}.d\vec{\sigma} - \iiint \vec{H}\frac{\partial \vec{B}}{\partial t} dV = \iiint \vec{E}.\frac{\partial \vec{D}}{\partial t}\, dV + \frac{dW_p}{dt} + \frac{dW_e}{dt} \tag{13S}$$

Where P is designated for the total applied power of pressure at time t, $\frac{dW_P}{dt}$ is the rate change of PE and $\frac{dW_e}{dt}$ is the rate change of EPE. The term $\iiint \vec{H}\frac{\partial \vec{B}}{\partial t}\, dV$ represents the energy that corresponds to the magnetic field and magnetization. Upon the removal of external pressure, the composite material undergoes relaxation, resulting in changes in elastic potential energy (EPE), potential energy (PE), electric energy, and electromagnetic field energy. As a result, an average electric potential ($\overline{V}$) is generated in the external circuit. Its magnitude remains the same during compression and recovery. Therefore, equation (14S) may be inferred as follows:

$$Q = \int I(t)dt - \int I(t_1)dt_1 = \frac{W_T - \hat{x}\iint \vec{S}d\vec{\sigma}dt - \hat{x}\iint \vec{S_o}d\vec{\sigma_o}dt_o -}{\overline{V}}$$

(14S)

Q represents the total charge that passes through the 3M PSCS device during compression and relaxation. $W_T$ denotes the cumulative work accomplished by the applied external force. Thus, as discussed, the electromagnetic field created on electrodes leads to the migration of $K^+$ and $OH^-$ ions in the direction of oppositely polarized electrodes, which in turn creates a concentration gradient and leads to the generation of open circuit potential. As the cyclic pressing process proceeds, the concentration of freely moving electrolytic ions at the electrode/electrolyte interface rises during compression and relaxation, resulting in the increased self-charging potential.

**Table S2.** Summary of recent research articles published in the field of externally controlled shielding applications

| Material system | Stimulation | Max. EMI Shielding (dB) | Ref. |
|---|---|---|---|
| PDMS/CZS/SWCNT/Iron fabric | Piezo-voltage | 87.8 | 6 |
| MXenes | Voltage | ~ 40 | 7 |
| PDMS)/FRS -RGO/ SWCNH | Mechanical pressure | ~35 | 8 |
| PDMS/SWCNT/Ag@Ni- Ionic liquid | Temperature/Mechanical pressure | 68.9/32.9 | 9 |
| CNT/LM/PDMS | Mechanical pressure | 42.2 | 10 |
| PDMS/CoZTO/SWCNT-Ethanol | Temperature/Mechanical pressure | 48.8 | 11 |
| G-RGO/NW-G | Humidity | 40 | 12 |
| PCT | Mechanical pressure | 43.4 | 13 |
| PDMS/SZTO/SWCNT-Water | Temperature | 50.4 | 14 |
| **3M PSCS Device** | **Self-Charging Potential** | **88.34** | **This work** |

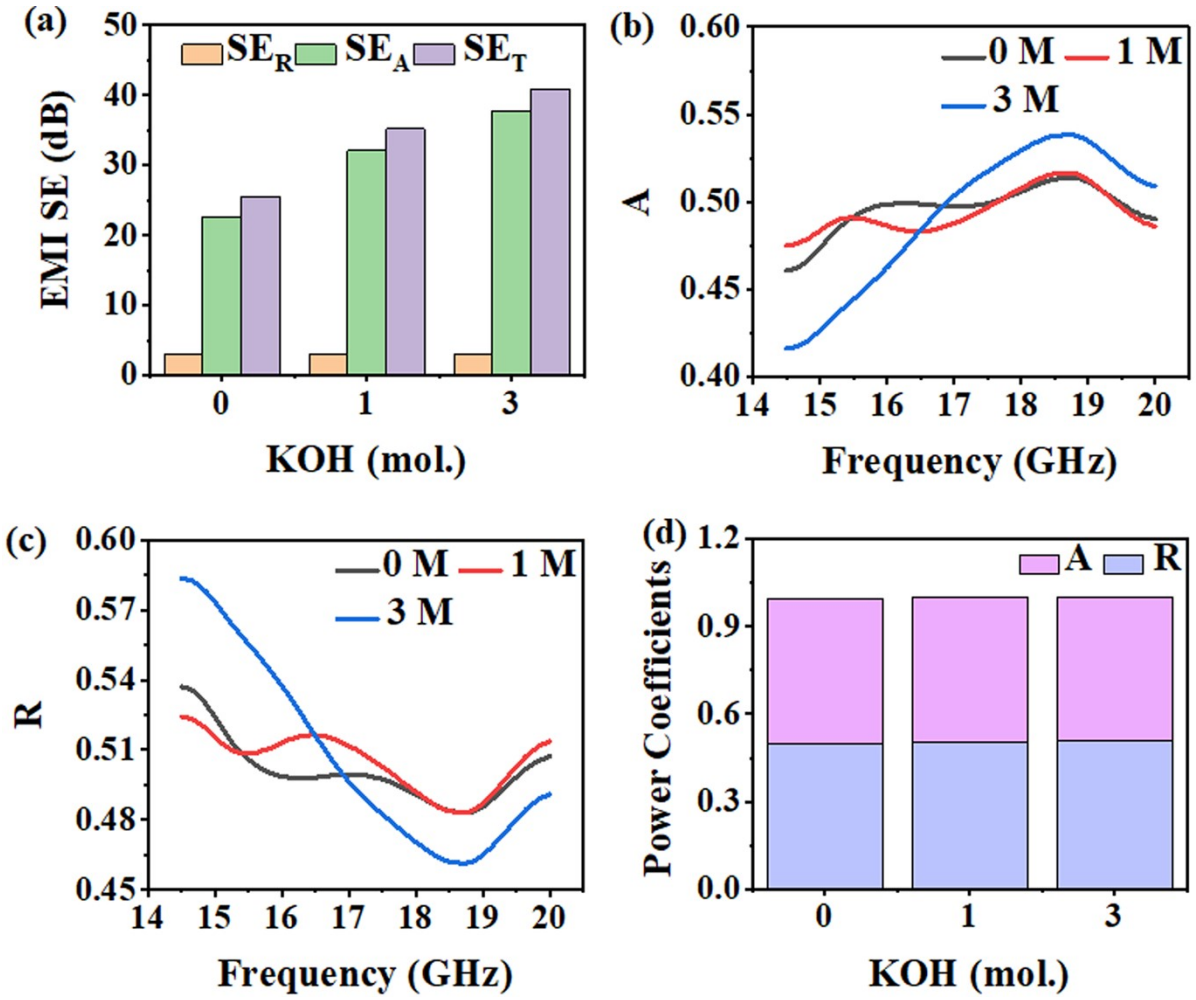


Fig. S7. (a) average $SE_T$, $SE_A$, $SR_A$, (b) A, (c) R, (d) average value of A and R.

**Table S3**. Variation of R, A, T with the KOH concentration in piezo electrolyte in PSCS devices.

| KOH Conc. | R | A | T |
|---|---|---|---|
| 0 | 0.50051 | 0.49671 | 0.00278 |
| 1 | 0.50482 | 0.49482 | 3.68695E-4 |
| 3 | 0.50703 | 0.49289 | 8.23946E-5 |

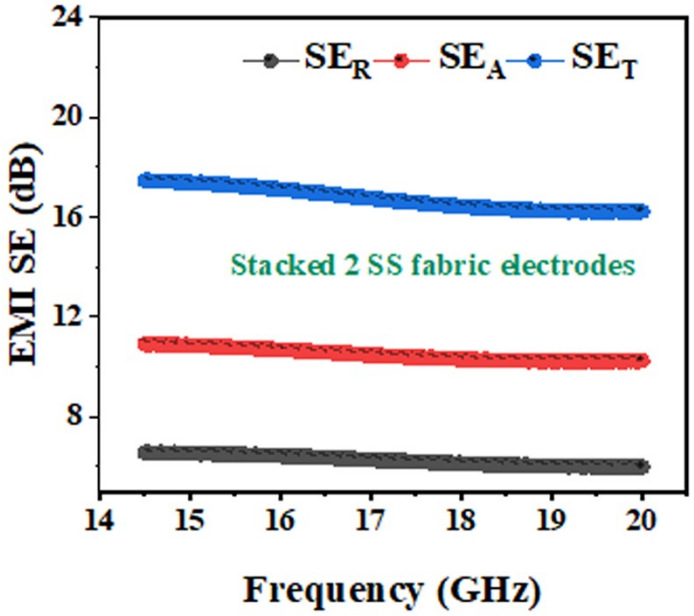


Fig. S8. $SE_T$, $SE_A$, and $SE_R$ of two SS fabric electrodes stacked over each other.

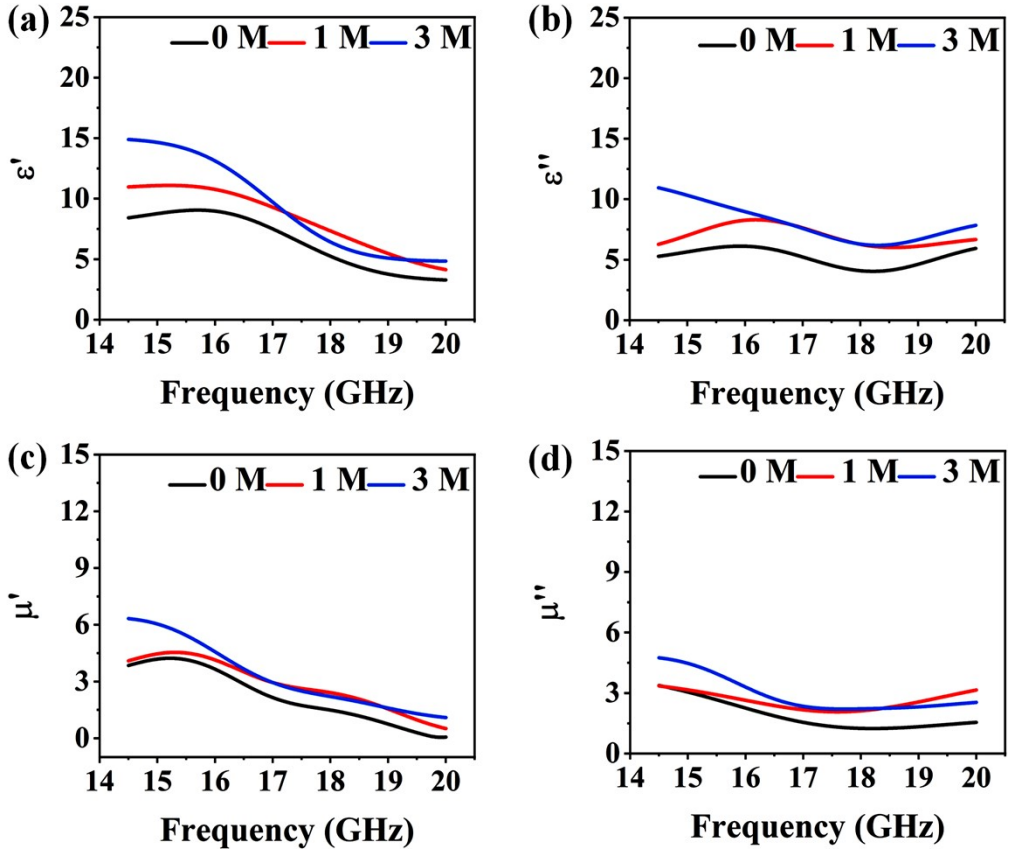


Fig. S9. Self-charging potential tuned: (a) real permittivity, (b) imaginary permittivity, (c) real permeability, (d) imaginary permeability.

## References


[1]. T. Lim, B.H. Seo, S.J. Kim, S. Han, W. Lee, J.W. Suk, *ACS Omega.,* 2024, **9(7)**, 8247-8254.

[2]. Y. Yan, B. Wu, C. Zheng, D. Fang, *Mater. Sci. Applications.,* 2012, **3(6),** 19835. DOI: 10.4236/msa.2012.36054.

[3]. S. Kumar, B.K. Satpathy, D. Pradhan, *Mater. Adv.,* 2024, **5(6),** 2271-2284.

[4]. A.A. AbdelHamid, A. Elgamouz, A.N. Kawde, *RSC Adv*., 2023, **13**, 21300-21312.

[5]. G. Maheshwaran, M.R. Prabhu, G. Ravi, K. Sankaranarayanan, S. Sudhahar, *Nano Energy.*, 2023, **106**, 108060.

[6]. P.P. Singh, A. Mondal, P. Maity, S. Ojha, G. Hati, B.B. Khatua, *Appl. Mater. Today.,* 2024, **36**, 102043.

[7]. M. Han, D. Zhang, C.E. Shuck, B. McBride, T. Zhang, R. Wang, K. Shevchuk, Y. Gogotsi, *Nat. Nanotech.,* 2023, **18**, 373–379.

[8]. R. Bera, A. Maitra, S. Paria, S.K. Karan, A.K. Das, A. Bera, S.K. Si, L. Halder, A. De, B.B. Khatua, *Chem. Engi. J.,* 2018, **335**, 501-509.

[9]. P.P. Singh, A. Mondal, P. Maity, B.B. Khatua, *J. Mater. Chem. C.,* 2023, **11(31)**, 10584 – 10597.

[10]. Y. Wang, Y.N. Gao, T.N. Yue, X.D. Chen, M. Wang, *Appl. Surf. Sci.,* 2021, **563**, 150255.

[11]. P.P. Singh, A. De, A. Mondal, P. Maity, B.B. Khatua, *Chem. Engi. J. Adv.*, 2023, **16**, 100568.

[12]. Y. Wang, X.D. Cheng, W.L. Song, C.J. Ma, X.M. Bian, M. Chen, *Chem. Engi. J.*, 2018, **344**, 342-352.

[13]. G. Wang, D. Yi, X. Jia, J. Chen, B. Shen, W. Zheng, *Mater. Today Phy.*, 2022, **22,** 100612.

[14]. P.P. Singh, A. De, B.B. Khatua, *Appl. Surf. Sci.,* 2024, **643**, 158643.